Available online at www.sciencedirect.com
ScienceDirect
Biosensors and Bioelectronics 22 (2007) 1466–1473
BIOSENSORS & BIOELECTRONICS
www.elsevier.com/locate/bios

Oxygen tolerance of an implantable polymer/enzyme composite glutamate biosensor displaying polycation-enhanced substrate sensitivity

Colm P. McMahon [a], Gaia Rocchitta [a,b], Sarah M. Kirwan [a], Sarah J. Killoran [a], Pier A. Serra [a,b], John P. Lowry [b], Robert D. O'Neill [a,*]

[a] *UCD School of Chemistry and Chemical Biology, University College Dublin, Belfield, Dublin 4, Ireland*
[b] *UCD School of Biomolecular and Biomedical Sciences, University College Dublin, Belfield, Dublin 4, Ireland*

Received 10 March 2006; received in revised form 17 June 2006; accepted 26 June 2006
Available online 2 August 2006

Abstract

Biosensors were fabricated at neutral pH by sequentially depositing the polycation polyethyleneimine (PEI), the stereoselective enzyme L-glutamate oxidase (GluOx) and the permselective barrier poly-*ortho*-phenylenediamine (PPD) onto 125-μm diameter Pt wire electrodes (Pt/PEI/GluOx/PPD). These devices were calibrated amperometrically at 0.7 V versus SCE to determine the Michaelis–Menten parameters for enzyme substrate, L-glutamate (Glu) and co-substrate, dioxygen. The presence of PEI produced a 10-fold enhancement in the detection limit for Glu (∼20 nM) compared with the corresponding PEI-free configurations (Pt/GluOx/PPD), without undermining their fast response time (∼2 s). Most remarkable was the finding that, although some designs of PEI-containing biosensors showed a 10-fold increase in linear region sensitivity to Glu, their oxygen dependence remained low.

Keywords: Glutamate oxidase; Polyethyleneimine; PEI; Poly(*o*-phenylenediamine); PPD; Michaelis–Menten; Brain monitoring; Neurochemistry

1. Introduction

The importance of L-glutamate (Glu) in systems as diverse as food processing and brain monitoring (O'Neill et al., 1998; Wilson and Hu, 2000; Wilson and Gifford, 2005; Dale et al., 2005; Fillenz, 2005) has led to intense interest in the development of sensors for this amino acid. In a neurochemical context, Glu is the main excitatory neurotransmitter, and a range of biosensor designs, based mainly on glutamate oxidase (GluOx; MW_r, 140 kDa; solution K_M, 0.21 mM in neutral buffer; p*I*, 6.2) (Kusakabe et al., 1983), have been described for direct monitoring of Glu in brain extracellular fluid (ECF) (Hu et al., 1994; Cosnier et al., 1997; Kulagina et al., 1999; Matsushita et al., 2000; Burmeister et al., 2003; Nickell et al., 2005; Rahman et al., 2005) (see reactions (1) and (2)). Encouraged by success in the design and application of an implantable biosensor for brain glucose (Lowry et al., 1994; Dixon et al., 2002), based on the immobilization of glucose oxidase (GOx) in a permselective polymer (poly-*ortho*-phenylenediamine, PPD) electrosynthesized in situ on Pt wire (Pt/GOx/PPD) (Sasso et al., 1990; Malitesta et al., 1990; Lowry and O'Neill, 1992; Wang and Wu, 1993; Bartlett and Birkin, 1994), this design has been adopted in recent years for the detection of ECF Glu (Pt/GluOx/PPD) (Ryan et al., 1997; Lowry et al., 1998b; McMahon and O'Neill, 2005).

The task of detecting brain ECF Glu, however, is significantly more challenging than glucose monitoring, mainly because the baseline ECF concentration of Glu appears to be ≤5 μM (Miele et al., 1996; Lada and Kennedy, 1996; Baker et al., 2002; Chen, 2005; Fillenz, 2005), although values as high as 15 μM have been suggested (Kulagina et al., 1999), and compares to ∼500 μM for ECF glucose (Boutelle et al., 1992; Lowry et al., 1998a). Thus, optimization of Glu sensitivity is critical for physiological applications, and we reported recently a significant enhancement of the linear region slope (LRS) for Glu, by incorporating the polycation polyethyleneimine (PEI) in these PPD-based biosensors (Pt/PEI/GluOx/PPD) (McMahon et al., 2006b).

$$\text{l-Glutamate} + H_2O + \text{GluOx/FAD} \rightarrow \alpha\text{-ketoglutarate} + NH_3 + \text{GluOx/FADH}_2 \quad (1)$$

* Corresponding author. Tel.: +353 1 7162314; fax: +353 1 7162127.
E-mail address: Robert.ONeill@UCD.ie (R.D. O'Neill).

0956-5663/$ – see front matter © 2006 Elsevier B.V. All rights reserved.
doi:10.1016/j.bios.2006.06.027

$$\mathrm{GluOx/FADH_2 + O_2 \rightarrow\ GluOx/FAD\ +\ H_2O_2} \quad (2)$$

$$\mathrm{H_2O_2 \rightarrow\ O_2 + 2H^+ + 2e} \quad (3)$$

The protein immobilizing agent (Tang et al., 1998) and stabilizer (Bryjak, 1995; Andersson and Hatti-Kaul, 1999), PEI, has been used previously in biosensors for a number of analytes, including Glu (Belay et al., 1999; Rahman et al., 2005; Varma et al., 2006). Studies suggest that PEI can have beneficial effects on biosensor performance by augmenting enzyme stability through the formation of polyanionic/polycationic complexes (Andersson et al., 2000) and by decreasing the electrostatic repulsion between the enzyme substrate and biosensor components (Chi et al., 1997; Jezkova et al., 1997; McMahon et al., 2006b). However, the enhanced sensitivity of oxidase-based biosensors to enzyme substrate, achieved using PEI, could have the undesired effect of greater sensitivity to changes in the concentration of co-substrate (O_2; see reaction (2)).

Since no literature is available on this topic, we investigate here the effects of incorporating PEI into Pt/GluOx/PPD biosensors on their oxygen dependence. The importance of oxygen interference in biosensor functionality is particularly relevant in applications involving in vivo monitoring, where pO_2 can fluctuate significantly (Clark et al., 1958; Bolger and Lowry, 2005). Thus, the suitability of a Glu biosensor design for a given application depends on the concentration of Glu being monitored, as well as the range of fluctuations in pO_2 relevant to that medium. For example, a combination of excessive Glu and low pO_2 could undermine the reliability of the Glu signal, and in extreme cases the biosensor becomes an oxygen sensor. The advantages and limitations of replacing O_2 in reaction (2) by various mediators has been discussed previously (O'Neill et al., 1998). Although these 'second generation' biosensors have the advantage of a low operating potential, they can suffer from a number of problems including leeching of untethered mediator from the enzyme layer, toxicity in biological tissues, and redox interference (e.g., oxidized ferrocenes can be reduced by ascorbic acid present in most biological media). Additionally, the complete insensitivity to oxygen tension sometimes claimed for mediated sensors has been questioned for certain mediators (Martens et al., 1995).

2. Materials and methods

2.1. Biosensor fabrication and calibration

Pt cylinders (Pt_C, 125 μm diameter, 1 mm length) were fabricated from Teflon®-coated Pt wire (Advent Research Materials, Suffolk, UK). GluOx (EC 1.4.3.11, 200 U mL^{-1}, Yamasa Corp., Japan) was deposited onto the metal surface by dip-evaporation (1–4 dips) (Ryan et al., 1997) and immobilized by amperometric electropolymerization (+700 mV versus SCE) in 300 mM *o*-phenylenediamine in phosphate buffered saline (PBS, pH 7.4) (Craig and O'Neill, 2003), as described previously to form Pt_C/GluOx/PPD biosensors (Ryan et al., 1997). Pt disks (Pt_D) were fabricated by cutting the Teflon®-coated wire transversely to produce 125 μm diameter disks, and Pt_D/GluOx/PPD biosensors were fabricated as for Pt_C. Additional sets of biosensors were prepared by pre-coating the Pt surface with the polycation polyethyleneimine (Aldrich, $MW_r \sim 750$ kDa, 1% aqueous solution), also by dip-evaporation, before enzyme deposition. The alternative polymer/enzyme configuration (enzyme deposited by dip-evaporation after the polymerization step) was also investigated: Pt_C/PPD/GluOx and Pt_D/PPD/GluOx, where the enzyme was immobilized by exposure to glutaraldehyde vapor (McMahon et al., 2005).

After rinsing and a settling period at 700 mV in fresh PBS, amperometric calibrations were carried out to determine the apparent Michaelis–Menten parameters (J_{max} and K_M(Glu); see below) and the linear region sensitivity (0–100 μM) of the biosensors to Glu and H_2O_2 in quiescent air-saturated buffer, unless stated otherwise. All electropolymerizations and calibrations were performed in a standard three-electrode glass electrochemical cell containing 20 mL quiescent PBS at room temperature. A saturated calomel electrode (SCE) was used as the reference electrode, and a large stainless steel needle served as the auxiliary electrode.

Experiments were computer controlled as described previously (Dixon et al., 2002; McMahon et al., 2005; McMahon et al., 2006b). Response times were recorded in constantly stirred solution, using a data acquisition rate of 100 Hz. A $t_{90\%}$ parameter was defined as the time taken for the analyte response to reach 90% of its maximum value from the start of the current upswing, and is similar to definitions used previously (Berners et al., 1994; Kulagina et al., 1999; Burmeister et al., 2003). The limit of detection (LOD) was determined using the widely applied criterion of three times the S.D. of the baseline.

2.2. Monitoring dissolved oxygen

A self-calibrating commercial membrane-covered amperometric oxygen sensor (CellOx 325 connected to an Oxi 340A meter, Carl Stuart Ltd., Dublin, Ireland) was used to quantify solution oxygen concentration as described previously (Dixon et al., 2002). This percentage was converted to an estimated concentration of O_2 by taking 200 μM to correspond to 100% (Bourdillon et al., 1982; Zhang and Wilson, 1993). To avoid contamination of the PBS by oxygen, the electrochemical cell was contained within an Atmosbag™ (Sigma) (Dixon et al., 2002). Oxygen sensor data and biosensor data were recorded simultaneously through the transition from N_2 saturation to air saturation. The biosensor response reached a plateau at oxygen levels which depended on the concentration of Glu in the cell, but typically by 30–50 μM O_2. Non-linear regression analysis of the current was performed up to this plateau region to determine the relevant $K_M(O_2)$ value (McMahon et al., 2006a; see Section 2.3).

2.3. Kinetic model and data analysis

A number of sophisticated mathematical models of the behavior of enzymes in membranes have been described (Albery and Bartlett, 1985; Bartlett and Pratt, 1993; Gooding et al., 1998; Phanthong and Somasundrum, 2003; Baronas et al., 2004). These complex analyses are often needed to understand and opti-

mize the behavior of thick and/or conducting layers (Gooding et al., 1998; Baronas et al., 2003). However, a recent study has shown that substrate diffusion is not limiting for PPD layers incorporating enzyme (De Corcuera et al., 2005), due to their relatively small thickness (Gooding et al., 1998). Therefore, the basic Michaelis–Menten enzyme parameters used here provide more readily accessible insights into factors affecting the responsiveness of biosensors fabricated from ultra-thin (10–30 nm; Malitesta et al., 1990; Sohn et al., 1991; Myler et al., 1997; Craig and O'Neill, 2003) insulating PPD, and avoids the use of more complex analyses, such as those involving the Thiele modulus (Gooding and Hall, 1996).

$$J_{Glu} = \frac{J_{max}}{1 + K_M(Glu)/[Glu]} \quad (4)$$

A two-substrate model is necessary to describe the kinetics of oxidase enzymes under conditions of varying concentration of both substrate and co-substrate (Leypoldt and Gough, 1984; Gooding and Hall, 1996). When the concentration of the co-substrate is constant, however, the two-substrate equation simplifies to the one-substrate Michaelis–Menten form (Eq. (4)), where the current density for the biosensor Glu response, J_{Glu}, is a measure of the overall rate of the enzyme reaction, and J_{max} is the J_{Glu} value at enzyme saturation. Different values of J_{max}, determined under the same conditions, reflect differences in the activity of enzyme on the surface (k_2[E]; see reaction (5)) (McMahon et al., 2005), provided the sensitivity of the electrode to H_2O_2 (reaction (3)) does not vary much, as is the case for the PPD-modified Pt cylinders and disks used here (Lowry and O'Neill, 1994; McMahon et al., 2004; McMahon et al., 2005).

$$E + S \underset{k_{-1}}{\overset{k_1}{\rightleftharpoons}} ES \xrightarrow{k_2} E + P \quad (5)$$

$$K_M = \frac{k_{-1} + k_2}{k_1} \quad (6)$$

The Michaelis constant, K_M, is defined in terms of the rate constants for the generalized reactions (reaction (5)) describing the conversion of substrate (S) to product (P), catalyzed by enzyme (E) (see Eq. (6)). When Eq. (4) is used to approximate the two-substrate case, the K_M is more complex, containing co-substrate terms. K_M is then the apparent Michaelis constant and phenomenologically defines the concentration of substrate that gives half the J_{max} response. Thus, changes in K_M are sensitive to the binding constant, k_1, and have often been interpreted in terms of barriers to substrate/enzyme binding (Sasso et al., 1990; Compagnone et al., 1996), as well as changes in oxygen demand (Zhang and Wilson, 1993).

$$J_{Glu} = \frac{J'_{max}}{1 + K_M(O_2)/[O_2]} \quad (7)$$

Alternatively, if the concentration of Glu is fixed and O_2 levels are changed, then Eq. (7) can be used to analyze the oxygen dependence of the Glu signal (Dixon et al., 2002; McMahon and O'Neill, 2005), where J'_{max} is the maximum (plateau) response for a particular concentration of Glu, and $K_M(O_2)$ is the apparent Michaelis constant for oxygen. The apparent Michaelis constant for Glu is useful for defining the linear range of Glu response ($(\sim 1/2)K_M(Glu)$), as well as the slope in the linear region, that is, LRS $\approx J_{max}/K_M(Glu)$ (see Eq. (8)).

$$\underset{[Glu]\to 0}{Lt}\, J_{Glu} = \frac{J_{max}}{1 + K_M/[Glu]} = \frac{J_{max}[Glu]}{[Glu] + K_M} \approx \frac{J_{max}}{K_M}[Glu] \quad (8)$$

Values of LOD, J_{max}, $K_M(Glu)$, LRS and $K_M(O_2)$ are presented as mean ± S.E.M., with n: number of biosensors; response times are reported as mean ± S.E.M., with n: number of electrodes x determinations. The statistical significance of differences observed between responses for the various designs was calculated using Student's two-tailed unpaired t-tests on the absolute current densities, slopes or Michaelis–Menten parameters.

3. Results and discussion

Recent studies have shown that the incorporation of PEI into PPD/GluOx-based biosensors led to a significant improvement in their performance, specifically a decrease in $K_M(Glu)$ and an increase in LRS (McMahon et al., 2006b). Before addressing the main aim of this investigation (the oxygen dependence of PEI-containing biosensors), the effects of PEI on other parameters (enzyme loading, response time and limit of detection) were determined to provide a fuller profile of the influence of this polycation on biosensor performance.

3.1. Response time and limit of detection

A number of properties of PPD-based biosensors indicate that their response is determined by enzyme kinetics, and not by diffusion through the polymer/enzyme composite (PEC) layer (see Section 2.3). In particular, their response time is fast (Lowry et al., 1994), being determined by the mixing time in stirred solution (Malitesta et al., 1990; Berners et al., 1994). To determine whether incorporation of large PEI molecules (~750 kDa, branched form) into the PEC matrix could thicken the enzyme-containing layer, and lead to diffusion effects in the biosensor response, response times ($t_{90\%}$) were measured for the four basic designs (see Fig. 1): Pt_C/GluOx/PPD (2.4 ± 0.2 s, $n = 24$); Pt_C/PEI/GluOx/PPD (1.7 ± 0.2 s, $n = 8$); Pt_D/GluOx/PPD (3.0 ± 0.2 s, $n = 46$); Pt_D/PEI/GluOx/PPD (2.4 ± 0.2 s, $n = 32$). There was therefore no slowing of the response times of PEI-containing devices, as has been observed for oxidase-containing biosensors involving thicker films such as redox hydrogels (~30 s) (Kulagina et al., 1999; Mikeladze et al., 2002; Castillo et al., 2005) and polypyrrole films (~1 min) (Malitesta et al., 1990; Yoshida et al., 1995). Indeed, PEI slightly decreased $t_{90\%}$ values for the corresponding geometry ($p < 0.05$).

The limit of detection was also improved by PEI. For cylinders: Pt_C/GluOx/PPD (0.31 ± 0.08 μM, $n = 8$) versus Pt_C/PEI/GluOx/PPD (0.02 ± 0.01 μM, $n = 4$, $p < 0.04$). For disks: Pt_D/GluOx/PPD (0.53 ± 0.04 μM, $n = 8$) versus Pt_D/PEI/

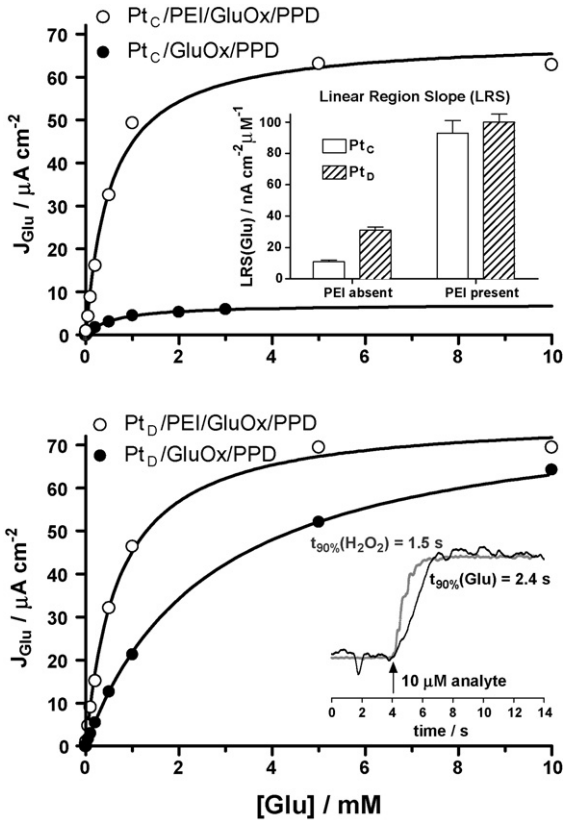

Fig. 1. Sample calibration data and non-linear regression analysis (Eq. (4)) for four biosensor designs: Pt$_C$/±PEI/GluOx/PPD (top) and Pt$_D$/±PEI/GluOx/PPD (bottom). Incorporation of polyethyleneimine (PEI) into biosensor fabrication increased the linear region slope (LRS = J_{max}/K_M (Eq. (8)); see top inset) for cylinders (by increasing J_{max}) and for disks (by decreasing K_M). See Fig. 2 for a scatter-plot analysis of K_M vs. J_{max} determined for 163 biosensors, and Table 1 for averaged values. The Glu response times ($t_{90\%}$; see bottom inset) in stirred solution were fast for all designs (<3 s); ~1 s of this was attributed to the enzyme reactions by comparing the $t_{90\%}$ values for H_2O_2 and Glu on the same sensors (see bottom inset).

GluOx/PPD (0.11 ± 0.02 µM, $n = 8$, $p < 0.0001$). These results are consistent with the greater LRS of the PEI-containing devices (Table 1) coupled with little or no increase in baseline noise, and contrasts with other sensitivity-boosting strategies, such as platinization (De Corcuera et al., 2005), that have little effect on limits of detection due to significant increase in baseline fluctuations.

3.2. Michaelis–Menten parameters for glutamate

Previous studies on the effects of PEI on PPD-based (McMahon et al., 2006b) and other designs of Glu biosensors (Rahman et al., 2005; Varma et al., 2006) focused on the apparent Michaelis constant (Eqs. (4) and (6)) and/or the linear region sensitivity. Here we report full calibrations for the determination of J_{max}, K_M(Glu) and LRS to understand more fully the beneficial effects of PEI on biosensor functionality, including oxygen dependence (see Section 3.4). Fig. 1 shows steady-state calibration points and non-linear regression (Eq. (4)) for individual examples of the four sensor configurations; Table 1 gives the mean ± S.E.M. values of Michaelis–Menten parameters for large populations of these biosensor types. PEI caused an eight-fold increase in J_{max} for cylinder-based electrodes, whereas there was a significant reduction (38%, $p < 0.04$) for disk values. The finding that PEI had opposite effects on J_{max} for cylinders and disks indicates that these changes are unlikely due to an effect on k_2, but instead result from an increase in enzyme loading ([E], reaction (5)) on cylinders and a decrease in [E] on the highly loaded disks. This explanation in terms of GluOx loading is consistent with the finding that the J_{max} values for PEI-containing cylinders and disks converged (see Table 1 and Fig. 2), with no significant difference between the two populations ($p > 0.1$).

The effect of PEI on K_M(Glu) was also different for disks and cylinders, as discussed elsewhere for a smaller population of biosensors (McMahon et al., 2006b). Here we present a more detailed correlation analysis for K_M(Glu) versus J_{max} for the four designs to probe these different PEI effects (see Fig. 2).

A useful index of active enzyme loading for these types of sensors is J_{max} (see Section 2.3). In the absence of PEI, J_{max} for cylinder devices fell within a narrow range (<20 µA cm^{-2}) and the K_M(Glu) values were relatively constant (see Fig. 2). This is consistent with the vertical dip-evaporation protocol used (1–4 dips) for deposition of the enzyme: the cylinder sides do not hold much solution at each dip, limiting the amount of GluOx deposited. For disks, however, the dome of solution produced by surface tension deposits a significantly greater density of GluOx on the Pt$_D$ surface. Thus, the range of J_{max} values for Pt$_D$/GluOx/PPD was larger (20–400 µA cm^{-2}), although Fig. 2 shows the data up to a maximum J_{max} value of 100 µA cm^{-2} to allow a clearer comparison with data for Pt$_C$/GluOx/PPD electrodes. Thus, in this analysis involving larger populations of

Table 1
Mean values ± S.E.M. for the two apparent Michaelis–Menten parameters (Eq. (4)), experimentally determined linear region slope (LRS), and the slope of $K_M(O_2)$ (Eq. (7)) vs. Glu concentration for each of four biosensor designs

	Components			
	Pt/GluOx/PPD		Pt/PEI/GluOx/PPD	
	Pt$_C$[a]	Pt$_D$[a]	Pt$_C$[a]	Pt$_D$[a]
J_{max} (µA cm^{-2})	8 ± 1 (55)	120 ± 12 (61)	61 ± 5 (27)	74 ± 6 (20)
K_M(Glu) (mM)	0.7 ± 0.1 (55)	4.3 ± 0.5 (61)	0.6 ± 0.1 (27)	0.6 ± 0.1 (20)
LRS (nA cm^{-2} µM^{-1})	11 ± 1 (55)	31 ± 2 (61)	93 ± 8 (27)	100 ± 5 (20)
$K_M(O_2)$ slope (µM O_2 µM Glu^{-1})	0.23 ± 0.02 (8)	0.06 ± 0.015 (13)	0.22 ± 0.01 (4)	0.13 ± 0.02 (4)

Number of biosensors in parentheses.
[a] Geometry.

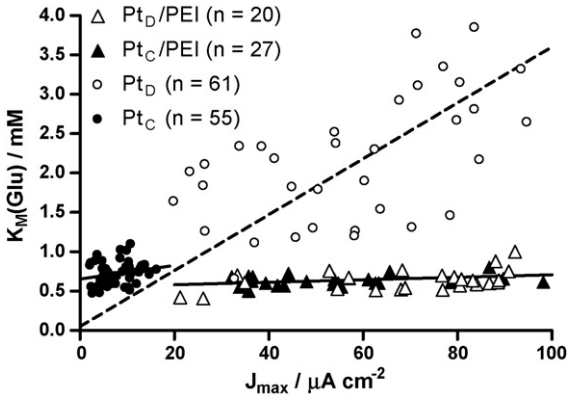

Fig. 2. Section of the scatter plots and linear regression for apparent Michaelis–Menten parameters (K_M(Glu) vs. J_{max} from Eq. (4)) for four biosensor designs fabricated by depositing the polymer/enzyme composite GluOx/PPD on either Pt_C, Pt_D, Pt_C/PEI or Pt_D/PEI (see Fig. 1 for examples of calibrations). The tendency for K_M(Glu) to increase with enzyme loading (J_{max}), especially for Pt_D-based devices ($R^2 = 0.82$; $p < 0.0001$), was abolished by PEI. Incorporation of PEI into the cylinder design increased J_{max} without increasing K_M(Glu), whereas PEI on disks decreased K_M(Glu) while maintaining a high J_{max} value. In effect, PEI led to convergence of the responses for the two geometries (see Table 1 for averages).

biosensors than in previous studies (McMahon et al., 2006b), differences between the disk and cylinder configurations are revealed (Fig. 2). The increased J_{max} for Pt_D/GluOx/PPD electrodes reflects a higher density of polyanionic enzyme on the surface, representing an electrostatic barrier to binding of the anionic substrate (at pH 7.4), which increases K_M(Glu) (McMahon et al., 2006b). However, the linear regression of this 'excess' K_M(Glu) (dashed line, Fig. 2) had an intercept of zero (0.1 ± 0.3 mM), showing that this crowding effect vanishes in the limit of zero GluOx coverage; what remained experimentally was the intrinsic K_M(Glu) for enzyme immobilized on Pt, namely the intercept displayed by Pt_C/GluOx/PPD electrodes (~0.6 mM).

Pre-coating the Pt with PEI had a significant effect on both cylinder and disk designs. Fig. 2 shows that PEI practically abolished the regression slope for disk-based biosensors (PEI absent, 36 ± 2, $n = 61$, $R^2 = 0.82$ versus 3 ± 1, $n = 20$, $R^2 = 0.24$ for PEI present). The correlation behavior of Pt_D/PEI/GluOx/PPD was similar to Pt_C/PEI/GluOx/PPD (slope $= 2 \pm 1$, $n = 27$, $R^2 = 0.29$), both possessing a K_M(Glu) intercept of 0.5 ± 0.1 mM Glu, which compares well with the low coverage value for Pt_C/GluOx/PPD biosensors. Thus, PEI did not significantly affect the interaction of Glu with GluOx when the enzyme molecules were widely separated (zero loading limit). This finding provides additional evidence that the effect of PEI is not mediated by diffusion effects through the PEI/GluOx/PPD matrix (see Section 3.1), and is consistent with our 'ultra-thin layer' enzyme kinetic analysis (De Corcuera et al., 2005).

3.3. Linear region slope for glutamate

Biosensors are usually designed to operate in real applications within their linear region of analyte response, which is generally considered to extend as far as $(1/2)K_M$. For biosensors incorporating GluOx, intended to detect low levels of Glu in biological samples, a critical property is high sensitivity in the linear region, whereas the range of linearity in not a problem. Since LRS $\approx J_{max}/K_M$ (Eq. (8)), increasing enzyme loading is a common strategy in the quest for increased LRS. The plot of LRS versus J_{max} in Fig. 3 shows, however, that the experimentally measured LRS did not increase with J_{max} for Pt_D/GluOx/PPD biosensors; Fig. 2 shows that the corresponding increase in K_M(Glu) for this design was the cause of the breakdown in this relationship (Eq. (8)). The incorporation of PEI into the PEC matrix restored this valuable correlation (Fig. 3), allowing significant increases in LRS mean values (Table 1).

3.4. Oxygen sensitivity studies

Biosensor oxygen dependence can be quantified as $K_M(O_2)$ defined by Eq. (7) (Dixon et al., 2002; McMahon and O'Neill, 2005; McMahon et al., 2005). The smaller the value of $K_M(O_2)$, the lower the oxygen dependence because higher oxygen affinity leads to oxygen saturation at lower pO_2, thereby reducing biosensor dependency at higher pO_2 levels. $K_M(O_2)$ is, phenomenologically, the concentration of oxygen at which the analyte signal is reduced to half its maximum value for a given concentration of analyte (see Fig. 4).

Fig. 4 shows the effect of changing the concentration of oxygen in the electrochemical cell, from sub-micromolar levels to 30 μM, on the biosensor signal recorded for 20 μM Glu, using two cylinder-based biosensors: Pt_C/GluOx/PPD and Pt_C/PEI/GluOx/PPD. Unexpectedly, the PEI-containing biosensor, with a nine-fold greater Glu sensitivity (LRS), showed a similar $K_M(O_2)$ value to the PEI-free device. Before attempting to explain this finding, the dependence of $K_M(O_2)$ on the

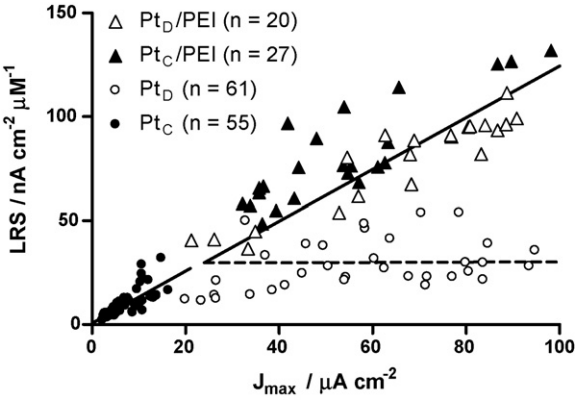

Fig. 3. Section of the scatter plots and linear regression analyses for the Glu calibration linear region slope (LRS) vs. J_{max} (Eq. (4)) for four biosensor designs fabricated by depositing the polymer/enzyme composite GluOx/PPD on either Pt_C, Pt_D, Pt_C/PEI or Pt_D/PEI (see Fig. 1 for examples of full calibrations). On bare Pt at low GluOx loading (J_{max}), i.e., for Pt_C, there was a systematic increase in LRS with J_{max} (slope $= 1.3 \pm 0.2$, $R^2 = 0.54$, $p < 0.0001$, $n = 55$). On bare Pt at higher GluOx loading, i.e., for Pt_D, there was no change in LRS with J_{max} (slope $= 0.01 \pm 0.02$, $R^2 = 0.003$, $p > 0.65$, $n = 61$). On Pt coated with PEI there was a systematic increase in LRS with J_{max} for both cylinders and disks (combined slope $= 1.2 \pm 0.1$, $R^2 = 0.49$, $p < 0.0001$, $n = 47$). Again (see Fig. 2), PEI led to convergence of the responses of the two geometries (see Table 1 for averages).

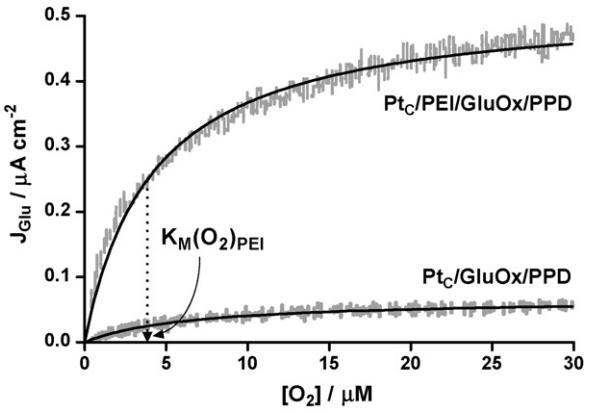

Fig. 4. Examples of raw data, recorded amperometrically (+700 mV vs. SCE) at 10 Hz with Pt_C/GluOx/PPD and Pt_C/PEI/GluOx/PPD biosensors, plotted against oxygen concentration recorded simultaneously using a CellOx sensor. The difference in the plateau currents illustrates the ~9-fold enhancement of the Glu sensitivity (LRS values; see Table 1) caused by PEI. The curve in each case represents the non-linear regression analysis, using Eq. (7). Surprising, the PEI-containing device with the higher Glu LRS did not show a higher oxygen dependence, $K_M(O_2)$; see arrow. The regression parameters obtained for these examples (20 μM Glu) were: $J'_{max} = 0.067 \pm 0.001$ μA cm^{-2}, $K_M(O_2) = 5.5 \pm 0.2$ μM, $R^2 = 0.92$ (Pt_C/GluOx/PPD), and $J'_{max} = 0.52 \pm 0.01$ μA cm^{-2}, $K_M(O_2) = 4.2 \pm 0.1$ μM, $R^2 = 0.98$ (Pt_C/PEI/GluOx/PPD). See Table 1 for averaged values.

concentration of Glu was determined for Pt/PEI/GluOx/PPD electrodes.

We established recently, for biosensors of the type Pt/GluOx/PPD, that $K_M(O_2)$ increases linearly with Glu concentration in the experimental range 5–150 μM Glu, with a limit of 0 μM oxygen as the concentration of Glu approaches zero (McMahon and O'Neill, 2005). The slope of these $K_M(O_2)$ versus Glu concentration plots defines the oxygen dependence of the sensor design in terms of micromolar oxygen per micromolar Glu (μM(O_2) μM(Glu)$^{-1}$). The $K_M(O_2)$ values were therefore determined, as in Fig. 4, over a range of Glu concentrations for biosensor incorporating PEI. Pt_C/PEI/GluOx/PPD electrodes showed a linear ($R^2 = 0.9999$) relationship between $K_M(O_2)$ and Glu concentration (4 biosensors × 3 concentrations) with an intercept that was not significantly different from zero (0.1 ± 0.1 μM O_2); Pt_D/PEI/GluOx/PPD electrodes also showed good linearity ($R^2 = 0.998$). However, the $K_M(O_2)$ regression slopes were different for these two sets ($p < 0.01$; see Table 1).

3.5. Relationship between $K_M(O_2)$ and $K_M(Glu)$

Oxygen demand of an oxidase-based biosensor (see reaction (2)) arises from the generation of the reduced form of the enzyme by substrate (reaction (1)). Thus, variations in $K_M(O_2)$ for different designs of the same basic biosensor type (Pt/±PEI/GluOx/PPD) are likely due to changes in some or all of the rate constants in reaction (5), and therefore in K_M(Glu) (Eq. (6)). The analysis in Section 3.2 suggests that changes in the binding of Glu (k_1, Eq. (6)) should play the most important part is the observed changes in K_M(Glu) (Fig. 2). To investigate this hypothesis, $1/K_M$(Glu) was used as a direct function of k_1 (Eq. (6)), and correlation analyses performed for mean values of $K_M(O_2)$ versus $1/K_M$(Glu) for the different designs. Since GluOx was deposited over large branched PEI molecules in some designs, and onto bare metal in others, it is possible that $K_M(O_2)$ could also have been influenced by additional routes of access by oxygen from below the enzyme in PEI-containing configurations. To control for this possibility, the $K_M(O_2)$ values for biosensors in which the GluOx was deposited over the PPD polymer and crosslinked with glutaraldehyde (Pt/PPD/GluOx) were included for comparison.

Fig. 5 shows the linear correlation ($R^2 = 0.990$, solid line) between $K_M(O_2)$ and $1/K_M$(Glu) for the populations of PEI-free biosensors. The intercept on the $K_M(O_2)$ axis was effectively zero, indicating that the oxygen dependence vanished as k_1 (Eq. (6)) approached zero, as expected (no H_2O_2 produced in reaction (2)). $K_M(O_2)$ increased steadily as k_1 increased over the entire range of J_{max} observed in this study (400 μA cm^{-2}). This again is expected as a result of an increase in the rate of H_2O_2 generation. Thus, this analysis is totally in line with expectation based on reactions (1) and (2).

Regression analysis between $K_M(O_2)$ and $1/K_M$(Glu) for the PEI-containing biosensors (Fig. 5) also gave a good linear correlation ($R^2 = 0.980$, dashed line). The intercept on the $K_M(O_2)$ axis was effectively zero, again indicating that the oxygen dependence vanished as k_1 approached zero. However, the regression slope was significantly less for biosensors with PEI (0.120 ± 0.007) compared with those without PEI (0.215 ± 0.008, $p < 0.0002$ for the difference in slopes). It appears therefore that PEI-containing PEC layers show a lower oxygen dependence than their PEI-free counterparts for a given value of k_1 (or K_M(Glu)). This is not likely due to the fact that

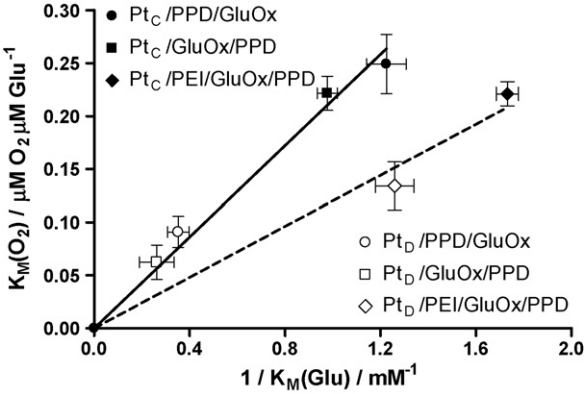

Fig. 5. Scatter plots and linear regression analyses for biosensor oxygen dependence, $K_M(O_2)$ slope (micromolar O_2 per micromolar Glu), vs. reciprocal of K_M(Glu), used as a measure of enzyme affinity for substrate, k_1 in Eq. (5) (see Eq. (6)). The behavior of PPD/GluOx and GluOx/PPD polymer/enzyme configurations is shown separately. Linear regression analysis for the four PEI-free biosensor configurations (solid line) showed good linearity (slope = 0.215 ± 0.008, $R^2 = 0.99$, $p < 0.001$) and a $K_M(O_2)$ intercept that was not significantly different from zero (0.009 ± 0.009 μM O_2). Similar analysis for the two PEI-containing biosensor configurations (dashed line) also showed good linearity (slope = 0.120 ± 0.007, $R^2 = 0.980$, $p < 0.005$) and a $K_M(O_2)$ intercept that was not significantly different from zero (-0.005 ± 0.021 μM O_2). Each point is a mean ± S.E.M.; see Table 1 for n-values ($K_M(O_2)$ data). For the two biosensor designs not included in Table 1 (Pt/PPD/GluOx), $n = 4$ in each case.

the enzyme is raised off the Pt surface when GluOx is deposited over PEI, because GluOx deposited over PPD (Pt/PPD/GluOx) did not show any deviation from the regression line defined by the opposite configuration (Pt/GluOx/PPD) (Fig. 5, solid line). This effect of reduced oxygen dependence of PEI-containing GluOx/PPD biosensors is clearly beneficial for their operation in environments where pO_2 fluctuates, such as in vivo applications. The mechanism is unclear, but might involve an increase in the affinity of the PEI-complexed GluOx/$FADH_2$ (reaction (2)) for oxygen.

4. Conclusions

Data for PEI-containing biosensors based on GluOx/PPD-coated Pt wire show that this polycation has several beneficial effects. There was up to a 10-fold decrease in the limit of detection for Pt_C/PEI/GluOx/PPD (∼0.02 μM Glu) with no adverse effect on response time (∼2 s). More importantly, in addition to the PEI-induced increase in linear region sensitivity reported recently (McMahon et al., 2006b), the oxygen dependence of Pt/PEI/GluOx/PPD biosensors has been determined and analyzed, and shown to be superior to that of the PEI-free configurations.

Acknowledgements

This work was funded in part by Science Foundation Ireland (03/IN3/B376 and 04/BR/C0198). We thank Dr. Kusakabe (Yamasa Corp., Japan) for a gift of glutamate oxidase, and Enterprise Ireland for a scholarship (CMcM).

References

Albery, W.J., Bartlett, P.N., 1985. J. Electroanal. Chem. 194, 211–222.
Andersson, M.A., Hatti-Kaul, R., 1999. J. Biotechnol. 72, 21–31.
Andersson, M.M., Hatti-Kaul, R., Brown, W., 2000. J. Phys. Chem. B 104, 3660–3667.
Baker, D.A., Xi, Z.X., Shen, H., Swanson, C.J., Kalivas, P.W., 2002. J. Neurosci. 22, 9134–9141.
Baronas, R., Ivanauskas, F., Ivanauskas, F., Kulys, J., 2004. J. Math. Chem. 35, 199–213.
Baronas, R., Ivanauskas, F., Kulys, J., 2003. Sensors 3, 248–262.
Bartlett, P.N., Birkin, P.R., 1994. Anal. Chem. 66, 1552–1559.
Bartlett, P.N., Pratt, K.F.E., 1993. Biosens. Bioelectron. 8, 451–462.
Belay, A., Collins, A., Ruzgas, T., Kissinger, P.T., Gorton, L., Csoregi, E., 1999. J. Pharmaceut. Biomed. Anal. 19, 93–105.
Berners, M.O.M., Boutelle, M.G., Fillenz, M., 1994. Anal. Chem. 66, 2017–2021.
Bolger, F.B., Lowry, J.P., 2005. Sensors 5, 473–487.
Bourdillon, C., Thomas, V., Thomas, D., 1982. Enzyme Microb. Technol. 4, 175–180.
Boutelle, M.G., Fellows, L.K., Cook, C., 1992. Anal. Chem. 64, 1790–1794.
Bryjak, J., 1995. Bioprocess Eng. 13, 177–181.
Burmeister, J.J., Palmer, M., Gerhardt, G.A., 2003. Anal. Chim. Acta 481, 65–74.
Castillo, J., Blochl, A., Dennison, S., Schuhmann, W., Csoregi, E., 2005. Biosens. Bioelectron. 20, 2116–2119.
Chen, K.C., 2005. J. Neurochem. 92, 46–58.
Chi, Q.J., Gopel, W., Ruzgas, T., Gorton, L., Heiduschka, P., 1997. Electroanalysis 9, 357–365.
Clark Jr., L.C., Misrahy, G., Fox, R.P., 1958. J. Appl. Physiol. 13, 85–91.
Compagnone, D., Federici, G., Bannister, J.V., 1996. Electroanalysis 7, 1151–1155.
Cosnier, S., Innocent, C., Allien, L., Poitry, S., Tsacopoulos, M., 1997. Anal. Chem. 69, 968–971.
Craig, J.D., O'Neill, R.D., 2003. Analyst 128, 905–911.
Dale, N., Hatz, S., Tian, F.M., Llaudet, E., 2005. Trends Biotechnol. 23, 420–428.
De Corcuera, J.I.R., Cavalieri, R.P., Powers, J.R., 2005. J. Electroanal. Chem. 575, 229–241.
Dixon, B.M., Lowry, J.P., O'Neill, R.D., 2002. J. Neurosci. Meth. 119, 135–142.
Fillenz, M., 2005. Neurosci. Biobehav. Rev. 29, 949–962.
Gooding, J.J., Hall, E.A.H., 1996. Electroanalysis 8, 407–413.
Gooding, J.J., Hall, E.A.H., Hibbert, D.B., 1998. Electroanalysis 10, 1130–1136.
Hu, Y., Mitchell, K.M., Albahadily, F.N., Michaelis, E.K., Wilson, G.S., 1994. Brain Res. 659, 117–125.
Jezkova, J., Iwuoha, E.I., Smyth, M.R., Vytras, K., 1997. Electroanalysis 9, 978–984.
Kulagina, N.V., Shankar, L., Michael, A.C., 1999. Anal. Chem. 71, 5093–5100.
Kusakabe, H., Midorikawa, Y., Fujishima, T., Kuninaka, A., Yoshino, H., 1983. Agric. Biol. Chem. 47, 1323–1328.
Lada, M.W., Kennedy, R.T., 1996. Anal. Chem. 68, 2790–2797.
Leypoldt, J.K., Gough, D.A., 1984. Anal. Chem. 56, 2896–2904.
Lowry, J.P., McAteer, K., El Atrash, S.S., Duff, A., O'Neill, R.D., 1994. Anal. Chem. 66, 1754–1761.
Lowry, J.P., O'Neill, R.D., 1992. Anal. Chem. 64, 453–456.
Lowry, J.P., O'Neill, R.D., 1994. Electroanalysis 6, 369–379.
Lowry, J.P., O'Neill, R.D., Boutelle, M.G., Fillenz, M., 1998a. J. Neurochem. 70, 391–396.
Lowry, J.P., Ryan, M.R., O'Neill, R.D., 1998b. Anal. Commun. 35, 87–89.
Malitesta, C., Palmisano, F., Torsi, L., Zambonin, P.G., 1990. Anal. Chem. 62, 2735–2740.
Martens, N., Hindle, A., Hall, E.A.H., 1995. Biosens. Bioelectron. 10, 393–403.
Matsushita, Y., Shima, K., Nawashiro, H., Wada, K., 2000. J. Neurotrauma 17, 143–153.
McMahon, C.P., Killoran, S.J., Kirwan, S.M., O'Neill, R.D., 2004. J. Chem. Soc. Chem. Commun., 2128–2130.
McMahon, C.P., Killoran, S.J., O'Neill, R.D., 2005. J. Electroanal. Chem. 580, 193–202.
McMahon, C.P., O'Neill, R.D., 2005. Anal. Chem. 77, 1196–1199.
McMahon, C.P., Rocchitta, G., Serra, P.A., Kirwan, S.M., Lowry, J.P., O'Neill, R.D., 2006a. Anal. Chem. 78, 2352–2359.
McMahon, C.P., Rocchitta, G., Serra, P.A., Kirwan, S.M., Lowry, J.P., O'Neill, R.D., 2006b. Analyst 131, 68–72.
Miele, M., Boutelle, M.G., Fillenz, M., 1996. J. Physiol. (Lond.) 497, 745–751.
Mikeladze, E., Schulte, A., Mosbach, M., Blochl, A., Csoregi, E., Solomonia, R., Schumann, W., 2002. Electroanalysis 14, 393–399.
Myler, S., Eaton, S., Higson, S.P.J., 1997. Anal. Chim. Acta 357, 55–61.
Nickell, J., Pomerleau, F., Allen, J., Gerhardt, G.A., 2005. J. Neural Trans. 112, 87–96.
O'Neill, R.D., Lowry, J.P., Mas, M., 1998. Crit. Rev. Neurobiol. 12, 69–127.
Phanthong, C., Somasundrum, M., 2003. J. Electroanal. Chem. 558, 1–8.
Rahman, M.A., Kwon, N.H., Won, M.S., Choe, E.S., Shim, Y.S., 2005. Anal. Chem. 77, 4854–4860.
Ryan, M.R., Lowry, J.P., O'Neill, R.D., 1997. Analyst 122, 1419–1424.
Sasso, S.V., Pierce, R.J., Walla, R., Yacynych, A.M., 1990. Anal. Chem. 62, 1111–1117.

Sohn, T.W., Stoecker, P.W., Carp, W., Yacynych, A.M., 1991. Electroanalysis 3, 763–766.
Tang, X.J., Xie, B., Larsson, P.O., Danielsson, B., Khayyami, M., Johansson, G., 1998. Anal. Chim. Acta 374, 185–190.
Varma, S., Yigzaw, Y., Gorton, L., 2006. Anal. Chim. Acta 556, 319–325.
Wang, J., Wu, H., 1993. Anal. Chim. Acta 283, 683–688.
Wilson, G.S., Gifford, R., 2005. Biosens. Bioelectron. 20, 2388–2403.
Wilson, G.S., Hu, Y.B., 2000. Chem. Rev. 100, 2693–2704.
Yoshida, S., Kanno, H., Watanabe, T., 1995. Anal. Sci. 11, 251–256.
Zhang, Y.N., Wilson, G.S., 1993. Anal. Chim. Acta 281, 513–520.